CORTEX 49 (2013) 1856–1873

Available online at www.sciencedirect.com

SciVerse ScienceDirect

Journal homepage: www.elsevier.com/locate/cortex

Research report

Abnormal network connectivity in frontotemporal dementia: Evidence for prefrontal isolation

Norman A.S. Farb [a,*], Cheryl L. Grady [a], Stephen Strother [a], David F. Tang-Wai [b,c], Mario Masellis [a,b,d], Sandra Black [a,b,d], Morris Freedman [a], Bruce G. Pollock [a,e], Karen L. Campbell [a,f], Lynn Hasher [a,f] and Tiffany W. Chow [a,b,e]

[a] Rotman Research Institute, Baycrest Centre, Toronto, Ontario, Canada
[b] Division of Neurology, University of Toronto, Toronto, Ontario, Canada
[c] University Health Network Memory Clinic, Toronto Western Hospital, Toronto, Ontario, Canada
[d] Sunnybrook Health Sciences Centre, Toronto, Ontario, Canada
[e] Centre for Addiction and Mental Health, Toronto, Ontario, Canada
[f] Department of Psychology, University of Toronto, Toronto, Ontario, Canada

ARTICLE INFO

Article history:
Received 7 December 2011
Reviewed 6 March 2012
Revised 1 June 2012
Accepted 14 September 2012
Action editor Robin Morris
Published online 24 September 2012

Keywords:
Frontotemporal dementia
Intrinsic connectivity networks
Resting state
Salience network
Systems neuroscience
Default network

ABSTRACT

Introduction: Degraded social function, disinhibition, and stereotypy are defining characteristics of frontotemporal dementia (FTD), manifesting in both the behavioral variant of frontotemporal dementia (bvFTD) and semantic dementia (SD) subtypes. Recent neuroimaging research also associates FTD with alterations in the brain's intrinsic connectivity networks. The present study explored the relationship between neural network connectivity and specific behavioral symptoms in FTD.

Methods: Resting-state functional magnetic resonance imaging was employed to investigate neural network changes in bvFTD and SD. We used independent components analysis (ICA) to examine changes in frontolimbic network connectivity, as well as several metrics of local network strength, such as the fractional amplitude of low-frequency fluctuations, regional homogeneity, and seed-based functional connectivity. For each analysis, we compared each FTD subgroup to healthy controls, characterizing general and subtype-unique network changes. The relationship between abnormal connectivity in FTD and behavior disturbances was explored.

Results: Across multiple analytic approaches, both bvFTD and SD were associated with disrupted frontolimbic connectivity and elevated local connectivity within the prefrontal cortex. Even after controlling for structural atrophy, prefrontal hyperconnectivity was robustly associated with apathy scores. Frontolimbic disconnection was associated with lower disinhibition scores, suggesting that abnormal frontolimbic connectivity contributes to positive symptoms in dementia. Unique to bvFTD, stereotypy was associated with elevated default network connectivity in the right angular gyrus. The behavioral variant was also associated with marginally higher apathy scores and a more diffuse pattern of prefrontal hyperconnectivity than SD.

Conclusions: The present findings support a theory of FTD as a disorder of frontolimbic disconnection leading to unconstrained prefrontal connectivity. Prefrontal

* *Corresponding author*. Rotman Research Institute, Baycrest Centre, 3560 Bathurst Street, Toronto, Ontario M6A 2E1, Canada.
E-mail address: nfarb@rotman-baycrest.on.ca (N.A.S. Farb).
0010-9452/$ – see front matter
http://dx.doi.org/10.1016/j.cortex.2012.09.008

hyperconnectivity may represent a compensatory response to the absence of affective feedback during the planning and execution of behavior. Increased reliance upon prefrontal processes in isolation from subcortical structures appears to be maladaptive and may drive behavioral withdrawal that is commonly observed in later phases of neurodegeneration.

1. Introduction

Frontotemporal dementia (FTD) includes an array of clinical syndromes characterized by the insidious onset of behavioral disinhibition and/or language impairment with commensurate degeneration of the frontal and anterior temporal lobes. The FTD syndrome consists of multiple subtypes: behavioral disinhibition in the behavioral variant of frontotemporal dementia (bvFTD) is typically associated with anterior foci of atrophy including the frontal lobe and ventral striatum. Language impairment due to progressive non-fluent aphasia and semantic dementia (SD) subtypes is more typically associated with temporal lobe atrophy (Seeley, 2010; Gorno-Tempini et al., 2011; Agosta et al., 2012). However, both behavioral and aphasic variants of FTD are distinguished by deficits in social cognition, motivation, and emotional awareness (Lavenu et al., 1999; Kipps and Hodges, 2006; Zamboni et al., 2008; Kumfor et al., 2011). Specifically, both bvFTD and SD patients exhibit clinically significant levels of emotion dysregulation, reducing the potential for social participation (Snowden et al., 2001; Merrilees et al., 2012). Since FTD selectively impairs affect and behavior regulation while leaving memory and visuospatial skills relatively intact, the study of altered brain function in FTD may clarify the regulatory neural mechanisms that promote adaptive social behavior. Such knowledge may also inform our understanding of FTD pathophysiology, potentially advancing diagnostic methodology and generating ideas for therapeutic intervention.

Progress in relating neurodegeneration to behavioral dysfunction has already been made through examinations of brain structure changes, relating atrophy of the ventral prefrontal cortex (PFC) and anterolimbic regions to symptom severity. In a study spanning several neurodegenerative diseases, disinhibition was associated with atrophy in the orbitofrontal cortex, anterior cingulate, and temporal lobes, whereas executive function was associated with preservation of the dorsal PFC (Krueger et al., 2011). In FTD, atrophy in the PFC and basal ganglia correlated with apathy, while atrophy of anterior limbic regions and temporal cortices correlated with disinhibition (Zamboni et al., 2008). In a bvFTD sample, apathy was associated with atrophy in both the frontal operculum and anterolimbic regions (Eslinger et al., 2012). In a rare functional imaging study of bvFTD, positron emission tomography (PET) imaging was used to link both apathy and disinhibition to reduced metabolic activity in the subgenual cingulate cortex (Peters et al., 2006). Presumably, the atrophy and metabolic decline of these frontal and limbic regions impact communication between brain regions leading to dysregulated behavior, but the functional brain changes underlying behavioral dysfunction have not been identified.

Beyond the revelation of structural differences, neuroimaging has the potential to identify subtle changes to brain networks underlying pathophysiology in processes critical to regulating behavior such as emotion processing (Davidson et al., 2002). However, a major challenge in investigating brain activity changes in FTD, and in dementia research in general, is ensuring patient comprehension and compliance with functional magnetic resonance imaging (fMRI) task paradigms. To this end, resting-state analysis has shown promise in uncovering the mechanisms of FTD and other dementias, as it allows for task-free estimation of the brain's intrinsic connectivity networks during fMRI acquisition (Greicius et al., 2004). Resting-state analysis identifies distinct networks of brain regions between which activity is correlated over time (Biswal et al., 1995; Lowe et al., 1998; Fox and Raichle, 2007), driven by low-frequency fluctuations (~.01–.1 Hz) in the blood oxygen-level dependent (BOLD) signal (Lowe et al., 2000; Cordes et al., 2001). The absence of task requirements has been particularly useful in the assessment of patients with dementia (Rombouts et al., 2005; Greicius, 2008; Koch et al., 2010).

To date there have been very few resting-state studies of FTD. These initial investigations reported pervasive changes to multiple resting-state networks, most notably a weakening of the salience network (SLN), a network bridging the frontal lobes and limbic system, characterized by communication between the anterior cingulate, insula, striatum and amygdala (Seeley et al., 2009; Zhou et al., 2010). Convergent findings have emerged from other imaging techniques: decreased metabolic activity in the SLN has been observed in FTD through ^{18}F-fluorodeoxyglucose PET (FDG-PET) (Peters et al., 2006; Foster et al., 2007; Gabel et al., 2010), and through arterial spin labeling (Du et al., 2006). Atrophy in the anterior insula atrophy is one of the earliest structural biomarkers of behavioral symptoms in FTD (Seeley, 2010), corroborating its significance in this functional network. In healthy individuals, the anterior insula appears to integrate emotional and visceral information into representations of present moment context that guide socially appropriate behavior (Farb et al., 2007; Seeley et al., 2007; Craig, 2009b; Wiech et al., 2010). Frontolimbic disconnection through the anterior insula is therefore a strong candidate mechanism for explaining behavioral symptoms in FTD.

Despite initial evidence of SLN dissolution in FTD, it remains unclear how generalizable these findings are across similar frontolimbic connectivity templates, or whether other intrinsic connectivity network changes also contribute to behavioral symptoms. For instance, Zhou et al. (2010) observed increased resting-state activity of a frontoparietal network, known as the 'default mode network (DMN)'. The DMN is composed of the posterior cingulate, precuneus, medial PFC, and angular gyri, and is associated with autobiographical memory and habitual, self-referential thought (Raichle et al., 2001; Greicius et al., 2003; Buckner et al., 2005). Both SLN and DMN changes may underlie behavioral dysregulation in FTD, as could any number of other local connectivity networks. In two recent meta-analyses

relating intrinsic connectivity networks to activation patterns in thousands of task-based neuroimaging experiments, several additional candidate networks for emotional and executive processing were identified (Smith et al., 2009; Laird et al., 2011). In particular, the 'executive network' as identified by Smith et al. was associated with both cognitive control and affective processing, encompassing both the executive and SLNs described in prior research (Seeley et al., 2007). This network provides a means for assessing frontolimbic connectivity, spanning anterolimbic, medial and dorsal PFC regions, measuring the integration of cognitive control in the dorsal PFC with limbic-driven behavioral impulses and affective tone. In addition to the executive network, Laird et al. (2011) identified five subcomponents networks associated with emotion, each of which could be used to test more thoroughly for changes to affective brain networks in FTD.

To explore changes to resting-state networks in bvFTD and SD, we employed multiple resting-state analysis techniques to probe for changes associated with disease status and severity. We primarily hypothesized that FTD would show disruptions to frontolimbic connectivity, and that these disruptions would predict behavioral dysfunction. As there have been few connectivity studies in FTD to date, we hoped both to replicate recent findings of altered connectivity networks such as the DMN and SLN, and to extend up on these findings by relating specific areas of connectivity change to behavioral impairment. In addition to an independent components analysis (ICA) of broad network connectivity, we sought to more precisely characterize local connectivity changes using several univariate techniques. To ensure that our findings were not simply the product of an arbitrary set of resting-state analysis methods, we also employed a host of alternative ICA network templates, in addition to a multivariate partial least squares (PLS) technique to replicate our findings, detailed in the Supplementary materials.

2. Methods

2.1. Ethics statement

All participants (or their substitute decision makers) provided informed consent according to the Canadian Tri-council Policy Statement on Ethical Conduct for Research Involving Humans, and the procedures were approved by the Research Ethics Board at Baycrest.

2.2. Participants

Sixteen participants with clinically diagnosed FTD and 16 healthy, age-matched control group participants (controls) were recruited to the study. Of the participants with FTD, eight had bvFTD, and eight had SD. Participant groups did not differ in age, gender or education, and FTD subgroups did not differ in symptom severity (Table 1; Supplementary Table 1 provides additional, individualized information).

2.3. Entry/inclusion criteria

Patients were recruited through the University of Toronto FTD Workgroup, which pools expertise from four tertiary care memory clinics across the city: Baycrest, the Centre for Addiction and Mental Health, Sunnybrook Health Sciences Centre and Toronto Western Hospital. At these centers, diagnoses are made on the basis of consensus between attending physicians from geriatric medicine, neurology or geriatric psychiatry, neuropsychologists, and speech and language pathologists. Each patient undergoing consensus diagnosis underwent comprehensive bedside neurological evaluation and neuropsychological examination, according to the standard batteries used in their referring clinics, although some SD patients demonstrated such severe aphasia that standard neuropsychological evaluation was impossible. Participants suspected of SD were furthermore referred for speech-language pathology assessments to confirm the semantic nature of their language impairments. For referral to the study, consensus was made that each patient had fulfilled the Neary et al. criteria either for bvFTD or SD (Neary et al., 1998).

Patients were referred to Dr. Chow for screening. To be included in the study, patients underwent screening for study eligibility, consisting of (1) a thorough review of the history of their present illness, and (2) prior structural magnetic resonance imaging (MRI) neuroimaging. Participants were also required to have a Clinical Dementia Rating (CDR) scale (Morris, 1993) total score < 3 and the ability to tolerate the MRI scanning environment. Concurrent neuropsychiatric medication was permitted, but only if it was at a stable dosing regimen for 3 months prior to the scan.

Table 1 – Participant demographic and clinical characteristics.

Variable	Controls ($n = 16$)	FTD participants	
		bvFTD ($n = 8$)	SD ($n = 8$)
Sex, M:F	9:7	4:4	4:4
Age, mean ± SE	67.2 ± 1.2	66.7 ± 2.5	64.5 ± 3.3
Education, mean ± SE	16.2 ± .5	16.0 ± .8	17.1 ± .9
FBI total score, mean ± SE	–	31.5 ± 4.5	21.2 ± 2.7[a]
FBI apathy score, mean ± SE	–	20.4 ± 2.7	13.9 ± 2.3[b]
FBI disinhibition score, mean ± SE	–	12.6 ± 2.7	8.1 ± 1.5
Stereotypy (SRI), mean ± SE	–	13.2 ± 3.2	10.8 ± 3.4
CDR, mean ± SE	–	1.6 ± .3	1.2 ± .2

a Significant ($p \leq .05$) difference between FTD subtypes.
b Marginal ($p \leq .1$) difference between FTD subtypes.

2.4. Exclusion criteria

Participants were excluded if they had a major medical illness in the past year or history of any neurological or psychiatric disorders which preclude diagnosis of FTD, including stroke, Parkinson's disease, alcoholism, head injury, major depression, or history of epilepsy. Controls were required to have a CDR score of 0, a Mini-Mental State Examination score of 27 or higher, a Shipley vocabulary score of 27 or higher, with no

significant history of neurological disease or structural pathology on MRI, and no neuropsychiatric medication.

2.5. Symptom measures

We employed several measures of FTD behavioral symptoms, with the goal of relating symptom severity to abnormalities in resting-state activity. Our primary measure was the frontal behavioral inventory (FBI) (Kertesz et al., 1997, 2000, 2003), which was developed to differentiate FTD from other neurodegenerative diseases. The 24-item scale is completed by the patient's primary caregiver, providing two 12-item subscales measuring apathy (negative symptoms) and disinhibition (positive symptoms), behavioral patterns common to FTD. To additionally characterize the additional symptom of rigid, repetitive behaviors often observed in FTD, we also employed the stereotypy rating inventory (SRI) (Shigenobu et al., 2002). In both the FBI and SRI, higher scores indicate greater levels of dysfunction.

2.6. Image acquisition

Images were acquired at Baycrest Hospital (Toronto, Canada) on a 3 T Siemens Magnetom Trio whole-body scanner with a matrix 12-channel head coil. Anatomical images were acquired using a magnetization-prepared rapid gradient echo pulse sequence as follows: repetition time (TR) = 2 sec, echo time (TE) = 2.63 msec, flip angle = 9°, matrix = 256 × 160, field of view (FOV) = 25.6 cm^2, slice thickness = 1 mm, 160 oblique axial slices, acquisition time = 6.5 min. Functional volumes were acquired using a T2*-weighted echo-planar image (EPI) pulse sequence as follows: TE = 30 msec, TR = 2000 msec, flip angle = 70°, acquisition matrix = 64 × 64, FOV = 20 cm^2. Thirty oblique axial slices of the brain were acquired at each time point with a voxel resolution of 3.1 × 3.1 × 5 mm. Participants were asked to lie with eyes closed during the resting-state acquisition run, during which 170 time points were collected.

2.7. Image pre-processing

2.7.1. Pre-processing

The first five frames of resting-state functional data were discarded to allow for magnetic field stabilization, yielding 165 time points of resting-state data for each participant. Following image reconstruction (SPM8 Digital Imaging and Communication in Medicine import utility; University College London, UK; http://www.fil.ion.ucl.ac.uk/spm/software/spm8), data were preprocessed using the Data Processing Assistant for Resting-State fMRI (DPARSF), an automated pipeline for resting-state fMRI data analysis based upon the Statistical Parametric Mapping (SPM) software package (Chao-Gan and Yu-Feng, 2010).

Participant time-series data were motion-corrected (translational motion parameters were less than one voxel for all included participants) and co-registered with their T1-weighted structural images. Each T1 image was bias-corrected and segmented using template (International Consortium for Brain Mapping) tissue probability maps for gray/white matter and cerebrospinal fluid (CSF). Warping parameters were obtained from the tissue segmentation procedure and subsequently applied to the time-series data (resampling to 3 mm^3 voxels). The time-series data were spatially smoothed using a 6 mm^3 full-width half maximum Gaussian kernel. The data were then linearly detrended and band-pass filtered to only include low-frequency fluctuations between .01 Hz and .1 Hz. Finally, we regressed out variance at each voxel associated with participant head motion parameters, as well as average white matter and CSF signal.

2.8. Broad network investigation through group ICA

Group spatial ICA was implemented using the Group ICA of fMRI Toolbox (GIFT) (version 1.3h; icatb.sourceforge.net) (Calhoun et al., 2001). The toolbox allows for the estimation of independent variance components at the group level by concatenating individual participant time courses together before estimation. Group ICA is performed in three main stages: first, the entire concatenated time course is reduced into a minimum number of principal components; second, the ICA algorithm is applied to determine independent components using orthogonal linear combinations of the original principal components; and finally, individual participant maps are reconstructed for each component.

Prior to the main analysis, we performed dimension estimation to determine the minimum description length, i.e., the minimum number of components required to explain variance in the data. In the present study, 44 independent components were estimated for the bvFTD group, 45 for the SD group, and 42 for controls. Following data reduction, the Fast ICA algorithm was used to identify components, in conjunction with the Icasso method for bootstrapping the ICA results to find the most consistent partitioning of the variance (Himberg et al., 2004; Correa et al., 2007). Icasso bootstrapping was performed 10 times to maximize independence of components. This analysis produced a set of spatial maps for each participant, with each map reflecting the global functional connectivity of a participant's brain voxels with a given independent component. The intensity values for these spatial maps were converted to z-scores to allow for comparisons between participants. Thus the product of the GIFT analysis was a set of spatial maps for each of the 32 participants, with each voxel value in the maps representing a connectivity score with that map's independent component.

Following the generation of individual participant maps, we employed an independently derived resting-state network template to identify the best-fitting ICA components. To assess frontolimbic connectivity, we selected Smith et al.'s "executive network" (Smith et al., 2009). The network was characterized using a binary template, thresholded at a z-score of $\geq$4.0 to reflect the spatial extent of resting-state networks identified in the resting-state literature (Damoiseaux et al., 2006).

To classify the participant component maps, we applied Seeley et al.'s automated template-matching algorithm to determine the best-fit network component map for each participant (Seeley et al., 2007, 2009; Zhou et al., 2010). To determine each component's goodness-of-fit, we applied the algorithm used in Zhou et al. (2010), multiplying (i) the average z-score difference of voxels falling inside − voxels falling outside the template; and (ii) the difference in the percentage of positive z-scores inside and outside the template. Each participant's best-fit component map was entered into the

group-level analysis, yielding a set of 32 images for the executive network connectivity template.

While we focus here upon the analysis of the executive network, we were able to extend our findings using the SLN and DMN templates described in prior research (Habas et al., 2009; Zhou et al., 2010). Convergent findings were also obtained by examining five emotion sub-network templates (Laird et al., 2011). Furthermore, SLN and DMN whole-brain connectivity differences in FTD were also replicated using PLS analysis a multivariate, seed-based technique (McIntosh and Lobaugh, 2004). All of these additional analyses and their results are described more fully in the Supplementary materials.

2.9. Local network investigation

We employed three additional techniques to attempt to identify local changes in network function that may drive the broad patterns of network changes observed through ICA: measures of voxel-wise signal power and homogeneity, and seed-based functional connectivity.

2.9.1. Fractional amplitude of low-frequency fluctuation (fALFF) analysis

Given the importance of low-frequency (i.e., .01–.1 Hz) fluctuations in determining resting-state activity, the analysis of low-frequency signal power has emerged as a fruitful approach to characterizing the local health of resting-state networks (Zou et al., 2008). At each voxel, low-frequency power is computed as the ratio of low-frequency power to the broader frequency spectrum of resting-state activity (i.e., 0–.25 Hz), thereby controlling for regions of high fluctuation that are not specifically low-frequency, such as vascular artifacts and high-frequency noise found in MRI susceptibility regions at the brain/CSF boundary. Low-frequency power was computed for each participant using the REST toolbox (Song Xiaowei, http://www.restfmri.net), yielding individual t-maps that were subsequently used in group-level analysis.

2.9.2. Regional homogeneity (REHO) analysis

REHO is a measure of local coherence in the brain, computed as the cross-correlation between each voxel and its neighbors (Zang et al., 2004). REHO has been successfully applied in differentiating resting-state activity between clinical and control groups, such as in patients with Alzheimer's disease (Liu et al., 2008) and autism (Paakki et al., 2010). The homogeneity signal is argued to represent local brain network integrity when applied to the analysis of the spontaneous low-frequency fluctuations observed during the resting-state (Zou et al., 2009). In the current study, we applied REHO as implemented in the REST toolbox, generating individual participant t-maps that were subsequently used in group-level analysis.

2.9.3. Seed-based univariate connectivity analysis

To better understand the impact of local network connectivity differences on whole-brain intrinsic connectivity networks, we investigated univariate connectivity, using a 'seed' region of interest (ROI) derived from the local network analysis. We defined a seed region using the conjunction region from the low-frequency power and REHO comparisons, reasoning that an area displaying abnormal local network activity may be indicative of changes to larger brain networks to which it is connected. For each participant, a whole-brain ROI connectivity map was generated using the REST toolbox and DPARSF. Fisher's Z-transformed maps were generated, allowing for tests of the whole-brain effects of seed connectivity across all participants, and the comparison of whole-brain seed connectivity between the bvFTD, SD, and control groups.

2.10. Group-level analysis of resting-state data

For each of the methods described above, the spatial maps of resting-state signal were entered into separate random-effects group analyses in SPM, allowing for between-group contrasts of signal strength at each voxel, as well as extraction of individual participant network correlation scores at each voxel. For each of the ICA-derived networks, we compared group-averaged levels of ICA network connectivity. For the local network analyses (low-frequency power and REHO), we compared group-averaged local network strength. Finally, for the univariate connectivity analysis, we compared group-averaged connectivity between the seed region and the rest of the brain. Comparisons were performed to establish differences common to both FTD variants versus controls, as well as to establish differences unique to each FTD variant versus the other variant and controls.

2.11. Brain-behavior analysis

To evaluate the relationship between resting-state network integrity and behavioral dysfunction in FTD, a covariate approach was employed. Individual patient scores on the FBI apathy, FBI disinhibition, and SRI scales were entered simultaneously as covariates in the analysis of variance (ANOVA) models used to compare the FTD groups and controls. To specify the covariates, patient scale scores were converted to z-scores (normalized across FTD participants) with control participants assigned a zero score. To illustrate the behaviorally relevant aspects of resting-state activity, significant covariates associations were displayed as parametric maps.

In a second approach, the most significant positive and negative contrast clusters from each analysis were used as ROIs to investigate the relationship between brain connectivity and symptom severity. From each ROI, the first eigenvariate characterizing the ROI signal was extracted using the MarsBar toolbox for SPM (http://marsbar.sourceforge.net), creating a vector of signal scores with one score for each participant. Signal scores from the FTD group were then subjected to pairwise correlation analyses with the apathy, disinhibition, and stereotypy scores. A simple (zero order) correlation analysis was performed across participants between resting-state scores and the three scales. Symptom severity was only measured within the FTD group, and was therefore orthogonal to the FTD versus control group contrast used to identify the ROIs. As this approach used an unbiased estimator of ROI location, it was suitable for reporting correlation values without violating assumptions of independence.

2.12. Correction for gray matter volume

To control for the confounding influences of gray matter atrophy on resting-state BOLD signal, we estimated voxel-wise gray matter intensity for each participant, and used these values as nuisance covariates in each of our analyses. We first estimated gray matter intensity using the voxel-based morphometry (VBM) toolbox for the SPM software package (VBM8; Wellcome Department of Imaging Neuroscience) (Ashburner and Friston, 2000), with default parameters. Structural images were tissue-classified into gray and white matter, and then DARTEL warped into a common space (Ashburner, 2007), including both linear and non-linear components in the estimation of the normalization model. The DARTEL normalization technique has been shown to produce comparable efficacy to manual volumetry when working with dementia populations (Mak et al., 2011). Anatomical images were created using only the non-linear components of the model, thereby controlling for the linear transformations of global brain size and orientation while displaying local, non-linear differences in gray matter volume. Modulated images were smoothed with a 6 mm full-width half maximum Gaussian kernel to create the final probability maps, matching the smoothness of the functional data. The bvFTD and SD groups were each separately contrasted against the controls using a one-way ANOVA.

To control for variations in gray matter volume, we employed the Robust Biological Parametric Mapping toolbox (Casanova et al., 2007; Yang et al., 2011). The toolbox uses robust regression to model the relationship between structural and functional data, controlling for influence by outliers and anatomical variation. The segmented gray matter maps from the VBM analysis were entered as nuisance covariates in all functional analyses.

2.13. Correction for multiple comparisons

All group-level analyses were performed in SPM8, using a random-effects ANOVA to model group-wide effects and contrast these effects between the FTD and healthy control groups. To characterize the gray matter differences in bvFTD and SD relative to controls, a family-wise-corrected $p < .05$ voxel height threshold was used. To increase sensitivity in functional analyses, a $p < .005$ voxel height threshold ($t \geq 2.75$) was used, in conjunction with a $p < .05$ family-wise-corrected cluster size threshold ($k \geq 70$–200 contiguous voxels depending on the analysis). Monte Carlo simulations suggested that these criteria were equivalent to family-wise error rate of $P_{FWE} < .01$ (AlphaSim, http://afni.nih.gov/afni/docpdf/AlphaSim.pdf). Behavioral symptom score covariates were also tested at this functional threshold.

To further reduce the potential for false positive results, all between-group comparisons of functional data were statistically thresholded using a very conservative conjunction approach (Friston et al., 1999, 2005), employed to identify group-specific network changes relative to the other two groups. For example, in investigating common FTD differences from controls, a conjunction of the contrasts (bvFTD *vs* controls) and (SD *vs* controls) was performed. In this conjunction, each contrast was required to be significant with correction for multiple comparisons, and then the overlap of these two contrasts needed to reach cluster size thresholds to be considered significant. To identify network differences unique to bvFTD, a conjunction of the contrasts (bvFTD *vs* controls) and (bvFTD *vs* SD) was applied, with a similar conjunction to identify unique SD differences. The effect of this conjunction approach was to lower the effective probability of type-I error at each voxel to a very conservative $p < 2.5 \times 10^{-5}$, while maintaining the family-wise-corrected cluster size threshold on the conjunction image.

3. Results

3.1. Clinical characteristics of the FTD groups

Neither of the FTD subgroups differed significantly from the control group or each other in demographic variables such as sex, age, or education (Mann–Whitney $U > 25$, *ns*). The average total FBI score across all patients was elevated [mean score ± standard error (SE) = 26.3 ± 2.9; Table 1 contains subgroup details], in keeping with prior reports of FTD (Kertesz et al., 1997), and supporting recent research suggesting that behavioral dysfunction is apparent in both FTD variants (Zamboni et al., 2008). The bvFTD demonstrated significantly higher FBI total scores than the SD group, $U = 12.5$, $p < .05$, with trends toward significance for each of the apathy ($U = 16.5$, $p = .10$) and disinhibition subscales ($U = 18.0$, $p = .14$), indicating greater behavioral dysfunction in the bvFTD group. Average patient stereotypy scores were also elevated across all patients (mean score ± SE = 12.0 ± 2.3) relative to established norms (Shigenobu et al., 2002), although the behavioral and aphasic variants did not differ from another ($U = 26.5$, *ns*).

Apathy and disinhibition were moderately correlated ($r_{14} = .57$, $p < .05$). Stereotypy was associated with both apathy ($r_{14} = .63$, $p < .01$) and disinhibition ($r_{14} = .57$, $p < .05$). None of the scales correlated with disease duration, as measured in years since symptom onset ($r_{14} \leq .31$, *ns*), and no behavior scores correlated with demographic variables.

3.2. Gray matter differences

Compared with healthy controls, both FTD subgroups showed widespread, left-lateralized reductions in gray matter volume, predominantly involving the insula, amygdala, and anterotemporal regions (Fig. 1). The bvFTD group showed additional atrophy in the right insula and the anterior cingulate, while the SD group showed more diffuse atrophy throughout the left anterior temporal lobe and ventral striatum. A complete list of bvFTD and SD atrophy locations relative to controls is available in Supplementary Table 2. Individual patient structural MRI slices are also available in Supplementary Fig. 1.

Behavioral covariate analysis with gray matter volume revealed two nearly overlapping patterns: gray matter volume reductions were associated with greater levels of apathy but lower levels of disinhibition throughout the medial prefrontal cortex and bilateral anterior insula, consistent with a correlation between advanced dementia behavioral staging and greater structural atrophy. Consistent with this interpretation, activity in the anterior cingulate peak of this covariate

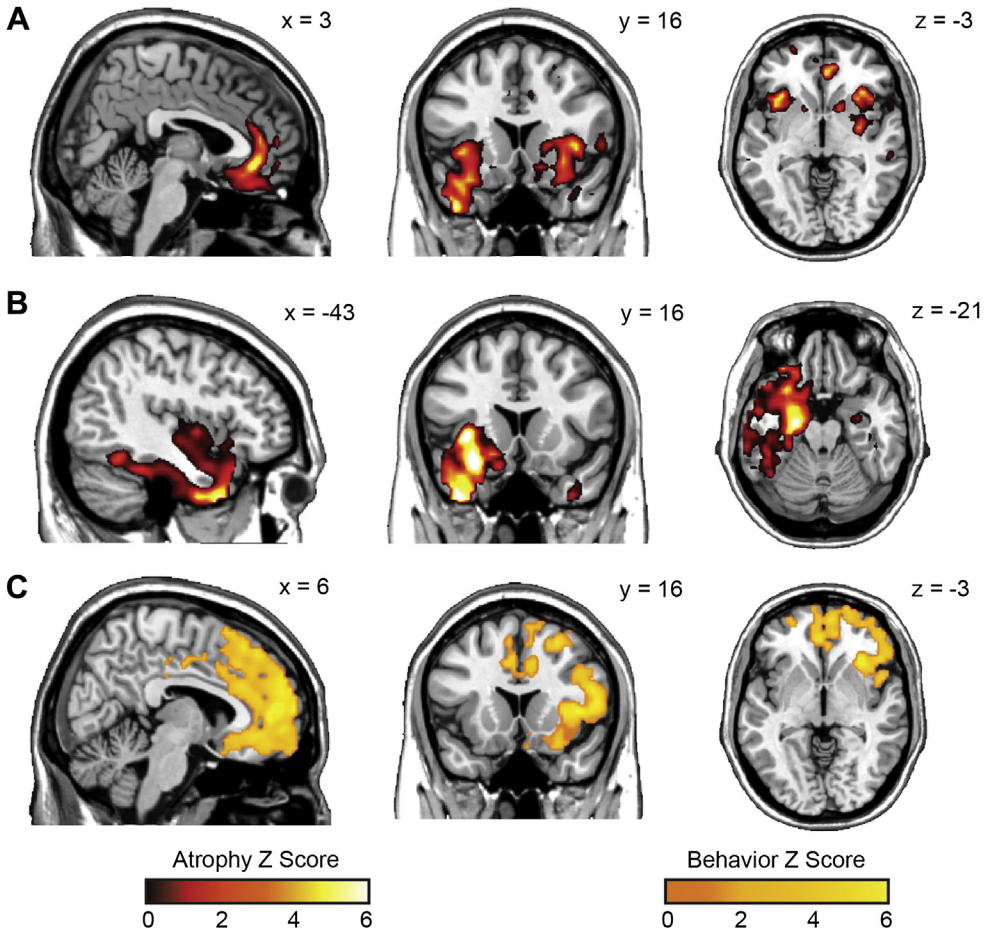

Fig. 1 – Group specific patterns of atrophy. Group-averaged gray matter maps were compared between the bvFTD group and controls (Panel A), and between the SD group and controls (Panel B). Panel C displays the conjunction of two covariates with patient gray matter densities: the positive covariates of disinhibition and the negative covariates of apathy. Thus the highlighted regions represent areas where gray matter atrophy is involved with reduced disinhibition and greater apathy.

map also demonstrated a strong association with CDR staging ($r_{14} = -.68$, $p < .005$).

3.3. *Resting-state network connectivity in FTD*

Executive network maps were first compared to identify abnormal connectivity patterns that were common to both FTD subtypes relative to controls (Fig. 2). Consistent with prior research, limbic connectivity was substantially reduced in both the bvFTD and SD groups, most notably in the insula, putamen, anterior thalamus, and middle cingulate cortex. However, we also observed a robust medial PFC cluster of elevated connectivity in both the bvFTD and SD groups. The behavioral covariate analysis revealed that both connectivity reductions in the anterior thalamus and elevated PFC connectivity were associated with greater levels of apathy.

Executive network maps were next examined to identify abnormal connectivity patterns that were unique to the behavioral and aphasic variants of FTD (Fig. 3). In bvFTD, more intense and diffuse prefrontal hyperconnectivity was observed relative to both SD and controls. Elevated connectivity was also observed in the posterior cingulate, generally regarded as an aspect of the DMN. Prefrontal hyperactivity unique to bvFTD was significantly associated with apathy ($r_{14} = .68$, $p < .005$) and marginally associated with disinhibition ($r_{14} = .44$, $p < .1$). By contrast, the SD group showed uniquely reduced executive network strength in the lateral PFC and anterior cingulate. These lateral PFC regions were also positively associated with apathy ($r_{14} = .64$, $p < .01$) and disinhibition ($r_{14} = .51$, $p < .05$), indicating that the absence of such connectivity in SD was protective, perhaps supporting reduced behavioral dysfunction in this aphasic subtype of FTD.

In additional analyses, we examined FTD-related connectivity changes in the SLN and DMN. The SLN analyses produced a pattern of results that were strikingly similar to the executive network analyses (Supplementary Fig. 2). Both the bvFTD and SD groups demonstrated reduced limbic connectivity and elevated prefrontal connectivity. The bvFTD group demonstrated a more diffuse pattern of elevated PFC connectivity than SD and controls. Contrary to the bvFTD group, the SD group demonstrated abnormally low connectivity in

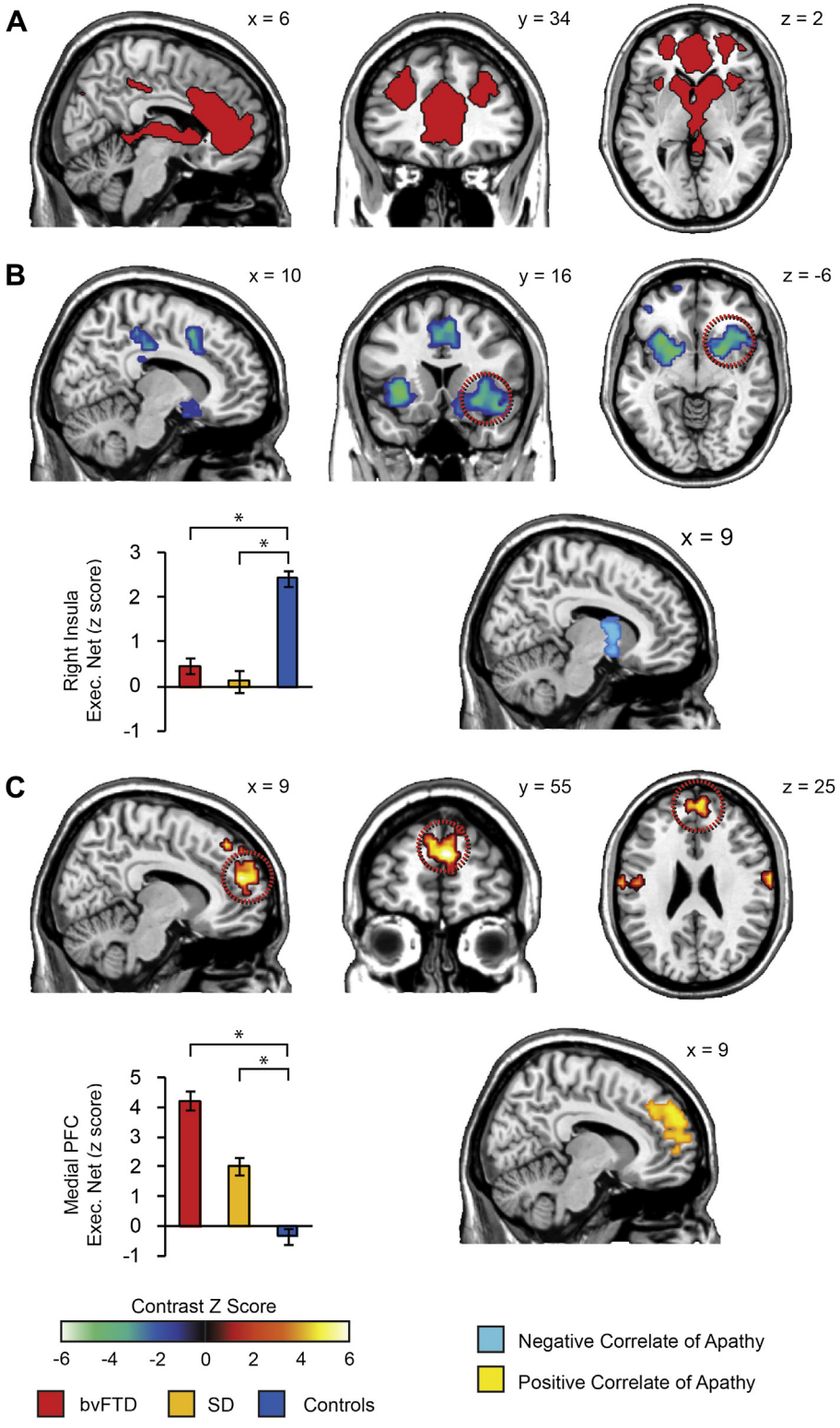

Fig. 2 – Abnormal executive network connectivity in FTD. Panel A depicts the executive network template from Smith et al. (2009). To conservatively estimate executive network changes common to both subtypes of FTD, we identified conjunction regions where both the bvFTD and SD subtypes demonstrated reduced (Panel B) and enhanced (Panel C) connectivity relative to controls. The bottom right regions of Panels B and C depict the executive network covariates of apathy, illustrating that both limbic disconnection and prefrontal hyperconnectivity are associated with higher levels of patient atrophy across FTD subtypes. Exec. Net = executive network.

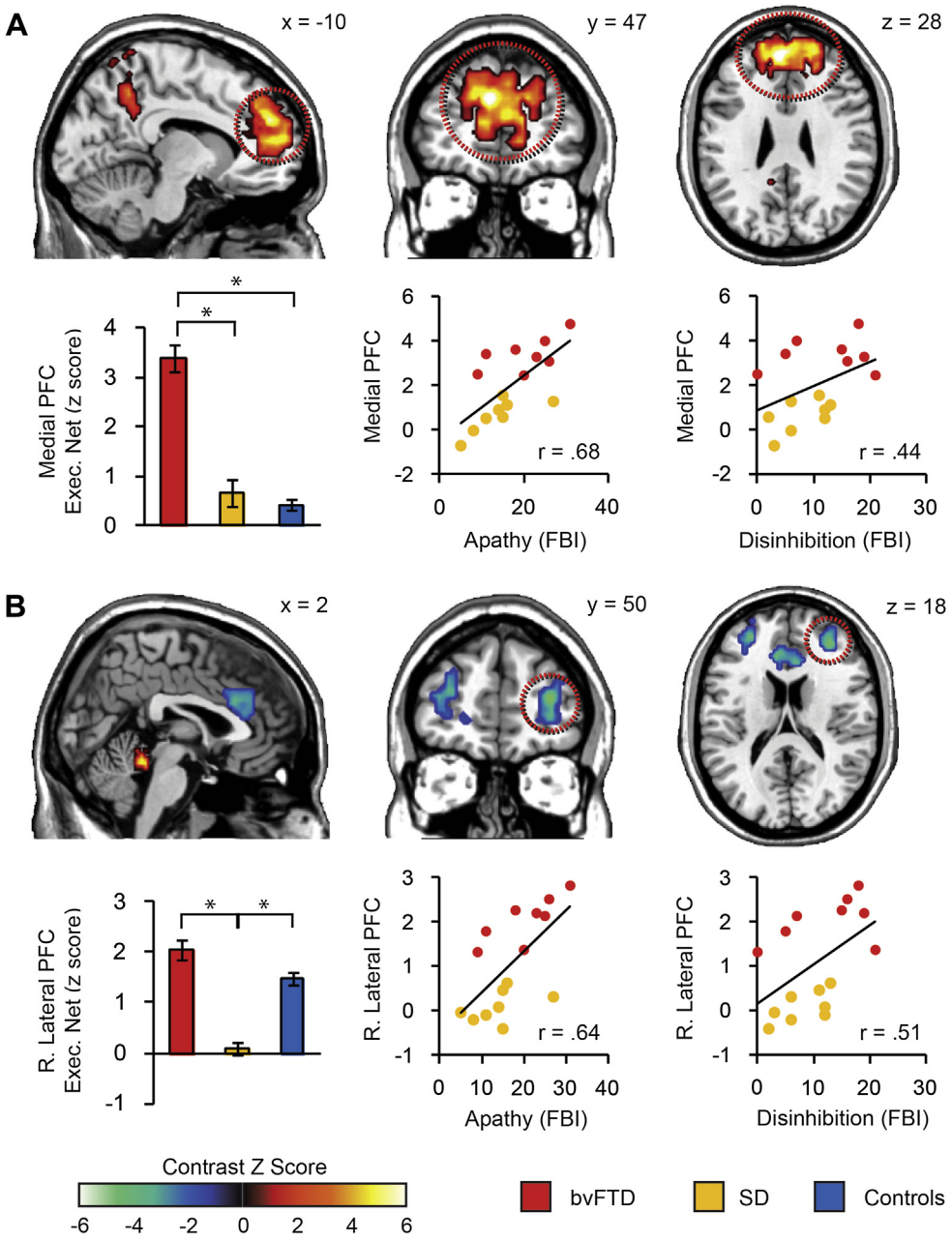

Fig. 3 – Abnormal FTD subtype specific executive network connectivity. Unique patterns of executive network connectivity were found in bvFTD compared to both SD and controls (Panel A) and in SD compared to both bvFTD and controls (Panel B). The peak regions in both of these comparisons demonstrated moderate associations with both atrophy and disinhibition. In bvFTD, elevated prefrontal connectivity is associated with more severe behavioral dysfunction, whereas in SD the absence of lateral prefrontal connectivity is associated with lower levels of behavioral dysfunction. Exec. Net = executive network.

the lateral PFC and anterior cingulate. Similar to the executive network analysis, elevated SLN connectivity in the PFC was associated with greater apathy (Fig. 4, Panel A). In addition, the SLN analysis yielded a positive association between reduced left insula connectivity and behavioral disinhibition, such that lower limbic connectivity also predicted lower levels of disinhibition (Fig. 4, Panel B). This finding is consistent with the hypothesis that limbic communication is required for disinhibition; without such communication, emotional impulses cannot influence behavioral control processes in the PFC.

The DMN analysis also revealed abnormal connectivity in FTD (Supplementary Fig. 3). Unique to bvFTD, increased connectivity was observed in the right angular gyrus relative to SD

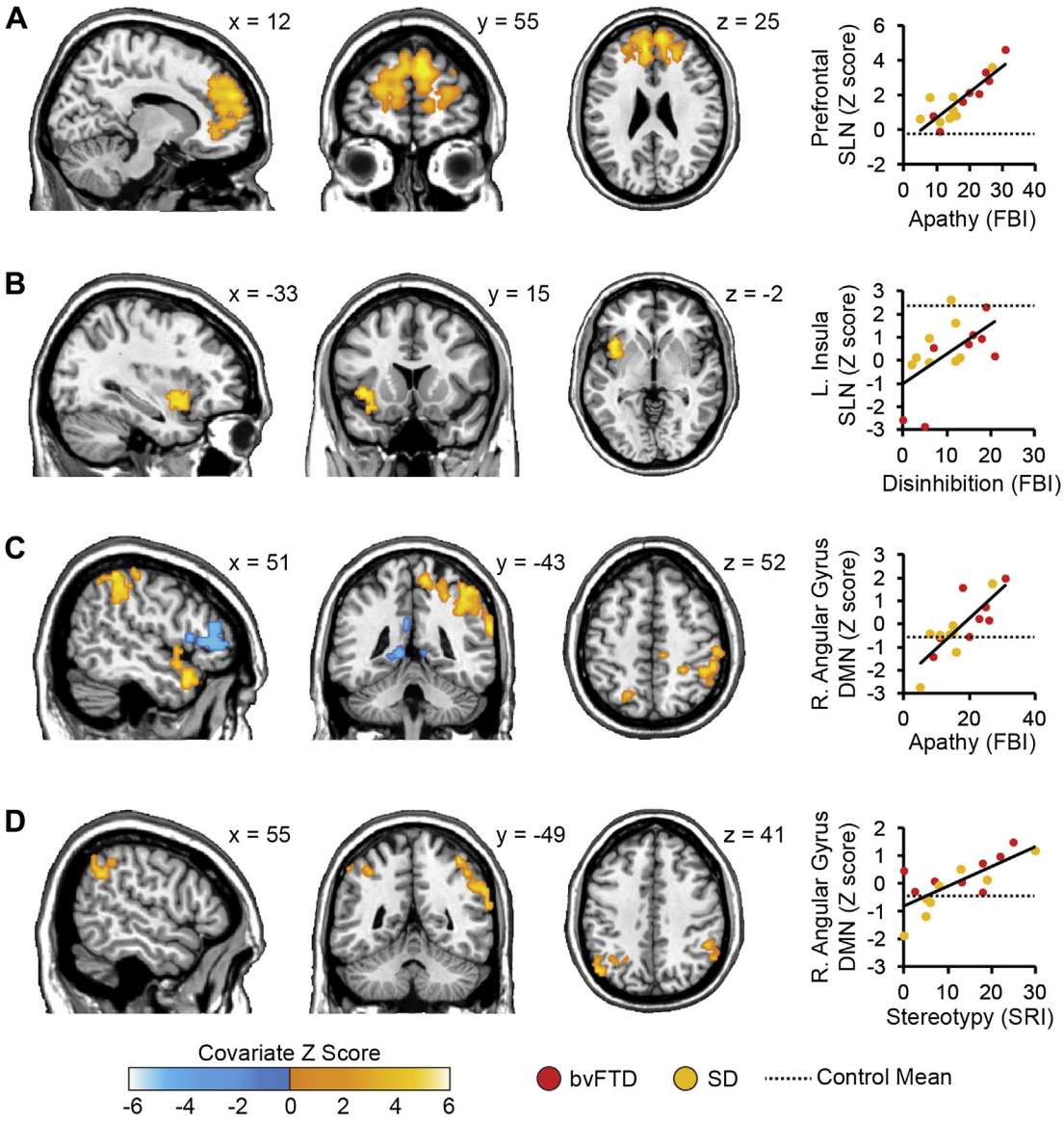

Fig. 4 – Covariates of behavioral dysfunction in the SLN and DMN. Several behavioral measures covary with patient SLN and DMN scores. Panel A: the covariates of apathy within the SLN. Panel B: the covariates of disinhibition within the SLN. Panel C: covariates of apathy in the default network. Panel D: covariates of stereotypy in the default network.

and controls. This elevated angular gyrus connectivity was associated with greater apathy and stereotypy scores (Fig. 4, Panels C and D). Additionally, both the bvFTD and SD groups demonstrated elevated connectivity with the left insula, a region traditionally associated with the SLN rather than the DMN.

Five emotion-related connectivity networks were further examined to provide a more comprehensive account of connectivity changes in FTD (Supplementary Fig. 4). Across these networks, reduced connectivity was observed between the PFC and the emotion networks: (1) the temporal network showed reduced connectivity with the dorsomedial PFC, (2) the subgenual network demonstrated reduced orbitofrontal connectivity, (3) the thalamic network had reduced subgenual connectivity, (4) the anterior insula and middle cingulate network demonstrated reduced connectivity with the anterior cingulate and lateral PFC, and (5) the cerebellum network lost connectivity with the thalamus and amygdala. From these five emotion networks, an interesting pattern of elevated connectivity also emerged. In the insula/cingulate network, prefrontal disconnection was balanced with the finding of elevated connectivity in the posterior insula, paralleling the PFC elevations observed in the executive and SLN analyses. A complete list of all between-group network differences are reported in Supplementary Tables 3–5.

3.4. *Local network differences*

Analyses of local network strength were performed to complement the broad network connectivity analyses (Fig. 5).

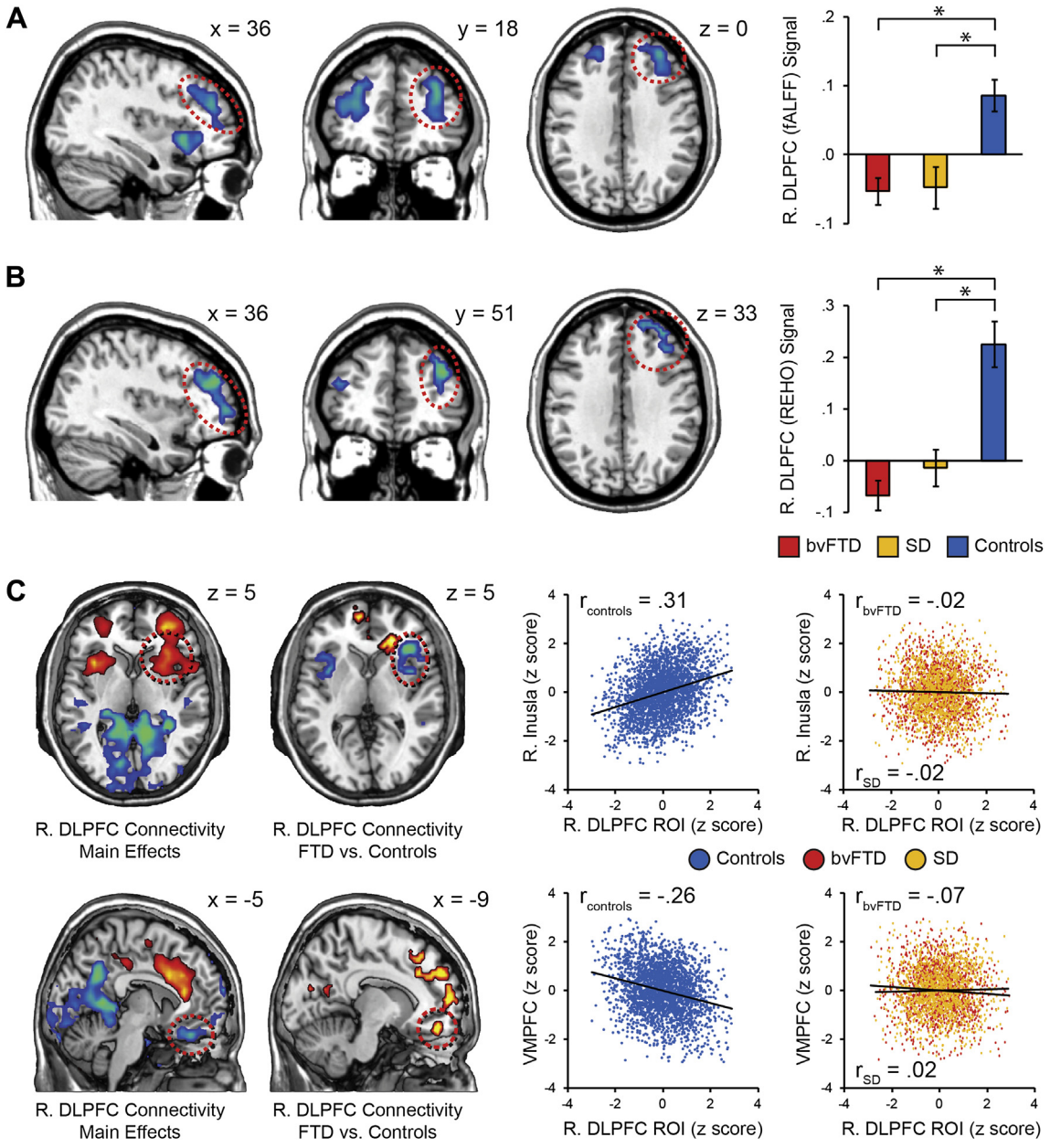

Fig. 5 – Univariate analysis summary. Panel A: using a conjunction analysis, the right insula and DLPFC demonstrated lower fALFF signal in both bvFTD and SD relative to controls. Panel B: conjunction analysis also revealed reduced DLPFC REHO signal in both bvFTD and SD relative to controls. Panel C: univariate connectivity results using the right DLPFC area common to the fALFF and REHO analyses as a seed region. The main effects shown bottom left demonstrate the overall pattern of functional connectivity from the DLPFC seed, which is positive correlated with the middle PFC and anterior insula, but negatively correlated with the VMPFC and posterior regions. The bottom middle demonstrates between-group differences in functional connectivity with the DLPFC, including decreased insula connectivity and increased VMPFC connectivity. Scatterplots display concatenated, z-scored data points from all participants, revealing that in both cases of altered connectivity, connectivity is present in controls but reduced to 0 in the two FTD subgroups.

Group comparisons showed that both the bvFTD and SD groups were associated with reduced low-frequency power in the right anterior insula and bilaterally in the dorsolateral PFC (DLPFC). Both the bvFTD and SD groups were also associated with reduced REHO bilaterally in the DLPFC as well as the cerebellum. A conjunction analysis revealed FTD-related reductions in both local network signals in bilateral DLPFC (BA 46; peak voxel $t_{1,30} = 4.33$; x = 36, y = 42, z = 30). The right DLPFC conjunction peak was then selected as seed region for connectivity analysis.

3.5. Seed-based connectivity

Across all participants, right DLPFC activity was positively correlated with the dorsal PFC and anterior cingulate, extending bilaterally into the anterior insula (Fig. 5, bottom left panel). This seed region was also negatively correlated with the posterior cingulate and ventromedial PFC (VMPFC). However, in comparisons against the control group, insula connectivity with the PFC was absent in both of the FTD groups. The negative connectivity observed between the DLPFC and VMPFC was also absent in both FTD groups (Fig. 5, bottom right panel).

Finally, to replicate our connectivity findings, we used a seed-based multivariate PLS approach. This analysis revealed very similar findings to the ICA approaches described above, with details available in the Supplementary materials.

4. Discussion

4.1. Summary of findings

Resting-state fMRI has the potential to improve our understanding of the neural networks underlying clinical manifestations of FTD, identifying pathways critical for the integration of emotional information in promoting adaptive behavior. The present study offers several important contributions: first, the data suggest that resting-state analysis can powerfully characterize intrinsic connectivity networks changes in FTD, validating accounts of SLN dysfunction in FTD (Seeley, 2010; Zhou et al., 2010). Second, we propose that FTD is a disorder of PFC hyperconnectivity in addition to frontolimbic disconnection, in which behavioral dysregulation may be driven by a removal of limbic constraints on PFC activity. Correlations with behavioral symptoms suggest that while some aspects of frontolimbic disconnection may reduce disinhibition, elevated PFC connectivity signals greater apathy, which contributes to dementia severity. Elevated posterior DMN connectivity also emerged as unique indicator of stereotypy. Together, these findings offer a more nuanced account of behavioral dysregulation in FTD, characterizing some positive and negative behavioral symptoms through their changes to distinct neural networks.

4.2. FTD as a disorder of frontolimbic connectivity

Reductions in frontolimbic connectivity were observed in both FTD variants, a finding that generalized across the executive and SLN templates. These networks model connectivity between the medial PFC and limbic system, extending from the anterior cingulate to the anterior insula, basal ganglia and striatum. Medial prefrontal and paralimbic regions are normatively connected through white matter tracts, most predominantly the antero-medial branch of the uncinate fasciculus (Thiebaut de Schotten et al., 2012). In the present structural analyses, the extent of subcortical gray matter atrophy suggests damage to these neighboring uncinate projections, a finding that has been directly observed in independent studies of FTD white matter integrity (Matsuo et al., 2008; Zhang et al., 2009).

Evidence of compromised communication was also evident along several more recently characterized white matter pathways. The insula is specifically connected to the frontal operculum through a series of U-shaped tracts that form the fronto-insular system (Catani et al., 2012) (Yeterian et al., 2012); seed-based connectivity analyses suggest a reduction in functional connectivity along this pathway (Fig. 5, top row of Panel C). The frontal aslant tract, recently characterized as an indicator of SLN integrity (Bonnelle et al., 2012), connects the anterior insula to the dorsal anterior cingulate (Thiebaut de Schotten et al., 2012). The present analyses showed evidence of reduced network coherence in this dorsal cingulate terminal of the aslant tract, suggesting that prefrontal isolation occurs along multiple connectivity pathways (Fig. 2, Panel B; Supplementary Fig. 2, Panel B). Furthermore, the seed-based connectivity analyses indicated that a ventral connectivity pathway between the PFC and limbic system also appeared to be compromised (Fig. 5, bottom of Panel C), consistent with reduced communication along the fronto-orbitopolar tract (Catani et al., 2012). As the characterization of the fronto-insular, fronto-orbitopolar and frontal aslant tracts is very recent, there is little evidence as to whether the tracts themselves are also compromised in FTD. Given that these connectivity deficits were apparent even after controlling for gray matter atrophy, white matter decline may be a good candidate for explaining these functional changes. Supplementary analyses supported this account of decline along multiple prefrontal pathways: the five emotion subcomponent networks demonstrated reduced connectivity between the PFC and a variety of surrounding affective brain regions.

Together, these disconnections point to a pervasive disruption in communication between the subcortical structures and the PFC. In functional terms, communication is compromised between affective and self-referential brain systems, consistent with clinical accounts of the disorder. While basic emotional responses may be preserved in FTD, the expression of more complex, self-referential emotions, such as embarrassment, is often compromised (Sturm et al., 2006; Werner et al., 2007). FTD patients have difficulty maintaining self-related goals (Miller et al., 2001; Harciarek and Jodzio, 2005), and are impaired in self-directed but not explicitly instructed emotion regulation (Goodkind et al., 2010). A lack of affective integration with conceptual self-reference may also account for the prevalence of socially inappropriate behaviors in FTD, as patients are unable to anticipate the feelings of others (Levenson and Miller, 2007).

Dysfunction with complex social emotions suggests a critical role for the PFC in FTD pathology, a region commonly associated with self-referential processing (Kelley et al., 2002; Goldberg et al., 2006). While PFC damage is generally associated with impairments in executive function (Manes et al., 2002), behavioral dysfunction in FTD may be related to the disease's unique pathology of targeting pathways of subcortical-PFC integration. Acting as a bridge between these regions, the ventral PFC may be particularly important for affect integration: Theory of Mind, the ability to predict the mental states and reactions of others, and is compromised in FTD (Freedman et al., 2012); this impairment is correlated with the extent of VMPFC atrophy (Gregory et al., 2002; Lough et al., 2006). As a counter-example, Huntington's patients, for whom atrophy is often constrained to subcortical rather than PFC regions, do not

typically demonstrate the same levels of emotional impairment found in FTD (Snowden et al., 2003, 2008).

A convergent finding in characterizing FTD as a disorder of frontolimbic connectivity was illustrated through the local network analyses. The right insula was identified as an area of both reduced low-frequency power and disrupted connectivity with the PFC, consistent with existing research implicating the right anterior insula in FTD pathophysiology (Seeley, 2010). The anterior insula features dense interconnectivity with the PFC via the proximal orbitofrontal cortex (Craig, 2003), theorized to help integrate visceral information into a broader motivational context (Critchley, 2005). If FTD atrophy first strikes this anterior insula region as has been theorized (Seeley, 2010), the ensuing reduction in low-frequency signal would significantly impair frontolimbic communication. The ability of the low-frequency analysis method to identify this right insula region in a whole-brain analysis is promising for its potential use as an early indicator of dementia pathophysiology, as the whole-brain ICA method did not demonstrate similar levels of anatomical specificity.

In addition to right insula dysregulation, FTD was also associated with reduced REHO and low-frequency power in the DLPFC (BA 46), a region long associated with the cognitive control of attention (Bunge et al., 2001) and particularly in the regulation of emotion (Pessoa, 2009). As directly confirmed through the seed-region connectivity analysis, the loss of REHO observed in the DLPFC provides converging evidence of disrupted communication from nearby limbic hubs such as the anterior insula, which acts as an indicator of emotional salience to direct attention and co-ordinate appropriate behavioral responses (Seeley et al., 2007; Menon and Uddin, 2010; Wiech et al., 2010).

These findings provide convergent evidence for the characterization of FTD as a disorder of frontolimbic connectivity. Taken broadly, the present results belie the notion that executive processes in the PFC, freed from emotional bias, might promote a more ordered and harmonious life. The clinical literature contains many parallel examples: frontolimbic disconnections have been associated with disordered behaviors found in psychosis (Filley and Gross, 1992), borderline personality disorder (Minzenberg et al., 2007; Salavert et al., 2011) and mania (Passarotti et al., 2011). While emotional biases on human decision making may lead to 'sub-optimal' performance on rational economic tasks, e.g., (Sanfey et al., 2003), these same emotional influences appear to be critical for adaptive social behavior.

4.3. *Elevated default mode connectivity in FTD*

The SLN holds particular importance for the allocation of attentional resources in response to the detection of emotionally salient events (Menon and Uddin, 2010), promoting transitions between internal and task-focused direction of attention (Sridharan et al., 2008). The dissolution of the SLN may therefore affect other networks, dysregulating dynamically competing systems responsible for the transition between mental states (Fox et al., 2005; Deco and Corbetta, 2011). For example, SLN activity appears to antagonistically modulate the DMN (Raichle et al., 2001; Sridharan et al., 2008). SLN degradation may therefore lead to stronger DMN connectivity (Zhou et al., 2010). Abnormally heightened DMN connectivity may in turn promote maladaptive behaviors driven by self-generated narratives and habit rather than what is emotionally salient and appropriate to environmental context (Farb et al., 2007).

The present results are consistent with this idea of SLN dysfunction promoting a maladaptively heightened DMN. Although the left insula is traditionally associated with the SLN, the DMN showed elevated left insula connectivity in both bvFTD and SD. In bvFTD specifically, greater default mode connectivity was also observed in the right angular gyrus, where elevated connectivity was associated with greater apathy and stereotypy scores. Associations with stereotypy were not observed as covariates of the other resting-state networks, consistent with the DMN's role in supporting habitual behavior and cognition. These findings also provide a cautionary tale against reliance upon habit without consideration of one's immediate motivational context; while automaticity supported by the DMN doubtlessly facilitates the performance of repetitive actions and mental operations, without emotional constraints, such automaticity is ill-suited for adaptively regulating behavior.

4.4. *FTD as a disorder of prefrontal hyperconnectivity*

Abnormally powerful and diffuse PFC connectivity was observed in both FTD subtypes, adding another dimension to existing accounts of FTD that focus on prefrontal disconnection. Relative to healthy controls, increased recruitment of the PFC was replicated across several network templates. For both the executive and SLNs, PFC hyperconnectivity was strongly associated with dementia severity, suggesting that this hyperconnectivity pattern was maladaptive rather than compensatory in nature.

The emergence of PFC functional hyperconnectivity may be better understood through reference to prefrontal structural connectivity. Much of the PFC is connected with sensory association and paralimbic cortex through bi-directional white matter pathways (Yeterian et al., 2012). The medial PFC (BA 32) normally connects to the temporal pole and insula through such pathways. Within the frontal lobe, the medial PFC demonstrates a greater dorsal than ventral trend in connectivity to dorsolateral prefrontal regions, consistent with the executive network template. In the absence of frontolimbic connectivity, the relatively spared fiber tracts within the PFC may give rise to increased local network activity. One might extrapolate from this finding that voxels in this prefrontal network demonstrate greater local coherence with their neighbors as complex afferent signal from limbic regions is lost; however, it should be noted that the REHO and low-amplitude analyses did not find any evidence of increased coherence or low-frequency power in the PFCs. Rather, it is likely that the broadened prefrontal coverage of the salience and executive networks observed in FTD reflects a consolidation of structurally connected prefrontal regions in the absence of competing connectivity from more limbic and posterior structures.

Extended connectivity throughout the dorsal PFC regions was a strong indicator of apathy in our FTD sample. FTD is commonly associated with difficulties in organization and

planning (Lindau et al., 2000; Merrilees and Miller, 2003), which require marshalling executive resources to bear on motivationally salient goals. Connectivity between dorsal and ventral regions appears to facilitate executive control during the performance of attention-demanding tasks (Seeley et al., 2007). Contextual feedback driving task initiation would normally recruit the SLN (Craig, 2009a), but because this pathway is impaired in FTD a compensatory monitoring system may be employed. Hyperconnectivity within the PFC may therefore reflect an attempt to marshal executive control processes; however, without access to motivational salience representations supplied by subcortical structures, such connectivity is insufficient to motivate goal-directed action. Additional executive control appears not to be an adequate substitute for motivational context, leading to apathetic behavior.

4.5. *Comparison of FTD variants*

The more dorsal and lateral aspects of PFC hyperconnectivity, typically reserved for executive processes rather than the self-referential and motivational functions (Seeley et al., 2007), were driven by the bvFTD group. Rather than performing executive processes such as selecting and maintaining task-relevant information, these executive networks appear to become conflated with more 'selfish' ventral PFC processes in bvFTD, leading to a degradation of cognitive control. This speculation is supported by the high associations observed between elevated dorsal PFC connectivity and higher levels of apathy and disinhibition. The same extent of diffuse PFC network recruitment was not evident in SD. The behavioral variant was also uniquely associated with elevated default mode connectivity that served as an indicator for apathy and stereotypy. Taken together, these findings characterize bvFTD as a disorder in which dorsal cortical regions become co-opted into resting-state networks, removing the competing contributions of cognitive control and automaticity to behavior. Instead, these unconstrained networks support repetitive action and apathetic internal-absorption that is characteristic of more advanced stages of the bvFTD.

By contrast, SD was associated with reduced dorsal and lateral PFC involvement in the executive and SLNs. This decline in executive PFC involvement may reflect a form of compensation for prefrontal isolation. Supplementary analyses of emotion networks suggested that SD was associated with elevated connectivity within the right insula and anterior temporal lobe, perhaps a compensatory recruitment in the face of pervasively atrophied left subcortical structures. This reliance upon right lateralized, and prosodic rather than syntactic language processes (Sammler et al., 2010) is consistent with observations of deficient emotional expression in the frontal-centered bvFTD, but excessive emotional expression in the limbic-reliant SD (Snowden et al., 2001). This distinction was also supported by the PLS supplementary analyses, which suggested that bvFTD promotes more local frontal connectivity but reduced sensory integration through limbic and posterior sensory networks; SD however was associated with stronger limbic connectivity but reduced integration of medial temporal and frontal networks. Future studies could explore whether this distinction between cortical disconnection in SD and limbic disconnection in bvFTD can be directly observed through white matter tract analytic methods such as diffusion tensor imaging (DTI) (Basser et al., 1994).

4.6. *Limitations*

The present analyses illustrate important neural network changes in FTD but bear limitations. First and foremost, due to a focus on broad network dynamics in our initial conceptualization of the project, we did not explicitly assess emotional comprehension or task planning to allow for fine-grained behavioral correlation with limbic and PFC network health. However, using the clinical measures employed, we were still able to relate these connectivity changes to behavioral dysfunction as perceived by caregivers on the FBI. A second limitation of this study is our small sample size in the bvFTD and SD groups; combined with our conservative conjunction analysis approach, a failure to detect differences between these groups might be due to low-study power. However, our ability to independently detect common areas of abnormal network connectivity in both subgroups relative to controls also lends credence to the power and pervasiveness of these changes in even a small cohort of patients.

Our findings are suggestive of changes to communication patterns in the brain, even after controlling for gray matter atrophy. However, without also analyzing white matter integrity, the degree to which such changes are the product of cortical reorganization versus white matter degradation is also unclear. Future studies investigating white matter integrity could also benefit from the recent characterization of white matter pathways bridging frontal and paralimbic regions, whose relative preservation and decline may help to better differentiate between different forms of behavioral and cognitive impairment in FTD.

An additional limitation to the study is the lack of uniform neuropsychological test data by which to classify patient diagnostic groups. Patients were referred to the study from a variety of different clinics, each employing a different set of measures in the assessment protocol. Thus, although all patients underwent a combination of neuropsychological and speech-language pathology evaluation as part of the consensus diagnosis process, it was not possible to simply aggregate test scores for comparison. Additionally, some SD patients had such severe aphasia that standard neuropsychological testing was impossible. Nevertheless, patient diagnosis proceeded through standard consensus criteria (Neary et al., 1998). Furthermore, when symptom severity did not preclude testing, speech-language pathology assessments were performed to differentiate cases of suspected SD from bvFTD. Despite these efforts, there were some cases in which overlapping behavioral and semantic symptoms were present; however, we believe that this overlap reflects a representative heterogeneity of symptoms among FTD patients, in which not all patients present with a diagnostically discrete cluster of symptoms. The present findings attempt to move beyond categorical classifications of FTD subtypes to look at common mechanisms of social dysregulation, providing insight into neural correlates of functional impairment rather than optimal diagnostic classification.

Finally, the present results offer provocative support for resting state analysis (RSA) as a complement to existing imaging procedures for dementia diagnosis. Larger research studies

will be needed to validate the utility of these findings in predicting FTD status, particularly due to our relatively small sample and lack of autopsy-confirmed cases. The hyper-recruitment of the frontal lobes for example was not observed in the first published study of resting-state analysis of FTD (Zhou et al., 2010), so it will be important to observe whether this hyper-recruitment is a consistent measure of FTD status, particularly at early phases of the disease. However, these novel findings are not likely due to the introduction of a different analysis pipeline, as the current findings were robust to a number of different resting-state templates and analysis methods, including a multivariate PLS analysis described in the Supplementary materials.

4.7. *Concluding remarks*

Changes to intrinsic connectivity networks in FTD appear to have important consequences for apathy, disinhibition, and stereotypy. Analyses of brain-behavior associations indicated that frontal hyperconnectivity was driven by patients with more severe symptoms, suggesting that this measure may be an indicator of disease progression rather than an early marker of FTD onset. Establishing a longitudinal model for the emergence of different indicators may aid our understanding of FTD etiology. Furthermore, the generalizability of these distinguishing effects must be examined to understand whether these resting-state metrics can be useful on a case-by-case clinical basis. Testing the predictive power of the network node locations in a larger, independent FTD population would provide stronger evidence for the clinical relevance of these measures. These limitations notwithstanding, our data offer an intriguing account of intrinsic connectivity network changes in FTD, relating symptoms of emotion dysregulation to both frontolimbic hypoconnectivity and dorsal PFC hyperconnectivity. Resting-state analysis techniques can provide important insights into how functional networks for emotional processing are compromised in FTD, insights which may eventually inform our understanding of behavioral symptoms and their potential resolution.

Acknowledgments

We gratefully acknowledge Bill Seeley and Helen Zhou for sharing resting-state network templates with us for the purpose of ICA. We thank the staff of the Baycrest MRI centre for technical assistance, and our patients, their families, and our healthy volunteers for their generous contribution to this research. This work was supported by the Canadian Institutes of Health Research (MOP89769 to LH; MOP14036 to CLG), the National Institute on Aging (F32AG022802 to TWC), the Women of Baycrest, and a gift from the Moir family. The funders had no role in study design, data collection and analysis, decision to publish, or preparation of the manuscript.

Supplementary data

Supplementary data related to this article can be found at http://dx.doi.org/10.1016/j.cortex.2012.09.008.

REFERENCES

Agosta F, Canu E, Sarro L, Comi G, and Filippi M. Neuroimaging findings in frontotemporal lobar degeneration spectrum of disorders. *Cortex*, 48(4): 389–413, 2012.

Ashburner J. A fast diffeomorphic image registration algorithm. *NeuroImage*, 38(1): 95–113, 2007.

Ashburner J and Friston KJ. Voxel-based morphometry – The methods. *NeuroImage*, 11(6 Pt 1): 805–821, 2000.

Basser PJ, Mattiello J, and LeBihan D. MR diffusion tensor spectroscopy and imaging. *Biophysical Journal*, 66(1): 259–267, 1994.

Biswal B, Yetkin FZ, Haughton VM, and Hyde JS. Functional connectivity in the motor cortex of resting human brain using echo-planar MRI. *Magnetic Resonance in Medicine*, 34(4): 537–541, 1995.

Bonnelle V, Ham TE, Leech R, Kinnunen KM, Mehta MA, Greenwood RJ, et al. Salience network integrity predicts default mode network function after traumatic brain injury. *Proceedings of the National Academy of Sciences of the United States of America*, 109(12): 4690–4695, 2012.

Buckner RL, Snyder AZ, Shannon BJ, LaRossa G, Sachs R, Fotenos AF, et al. Molecular, structural, and functional characterization of Alzheimer's disease: Evidence for a relationship between default activity, amyloid, and memory. *Journal of Neuroscience*, 25(34): 7709–7717, 2005.

Bunge SA, Ochsner KN, Desmond JE, Glover GH, and Gabrieli JD. Prefrontal regions involved in keeping information in and out of mind. *Brain*, 124(Pt 10): 2074–2086, 2001.

Calhoun VD, Adali T, Pearlson GD, and Pekar JJ. A method for making group inferences from functional MRI data using independent component analysis. *Human Brain Mapping*, 14(3): 140–151, 2001.

Casanova R, Srikanth R, Baer A, Laurienti PJ, Burdette JH, Hayasaka S, et al. Biological parametric mapping: A statistical toolbox for multimodality brain image analysis. *NeuroImage*, 34(1): 137–143, 2007.

Catani M, Dell'acqua F, Vergani F, Malik F, Hodge H, Roy P, et al. Short frontal lobe connections of the human brain. *Cortex*, 48(2): 273–291, 2012.

Chao-Gan Y and Yu-Feng Z. DPARSF: A MATLAB toolbox for "Pipeline" data analysis of resting-state fMRI. *Frontiers in Systems Neuroscience*, 4: 13, 2010.

Cordes D, Haughton VM, Arfanakis K, Carew JD, Turski PA, Moritz CH, et al. Frequencies contributing to functional connectivity in the cerebral cortex in "resting-state" data. *American Journal of Neuroradiology*, 22(7): 1326–1333, 2001.

Correa N, Adali T, and Calhoun VD. Performance of blind source separation algorithms for fMRI analysis using a group ICA method. *Magnetic Resonance Imaging*, 25(5): 684–694, 2007.

Craig AD. Interoception: The sense of the physiological condition of the body. *Current Opinion in Neurobiology*, 13(4): 500–505, 2003.

Craig AD. Emotional moments across time: A possible neural basis for time perception in the anterior insula. *Philosophical Transactions of the Royal Society London B Biological Science*, 364(1525): 1933–1942, 2009.

Craig AD. How do you feel–now? The anterior insula and human awareness. *Nature Reviews Neuroscience*, 10(1): 59–70, 2009.

Critchley HD. Neural mechanisms of autonomic, affective, and cognitive integration. *Journal of Comparative Neurology*, 493(1): 154–166, 2005.

Damoiseaux JS, Rombouts SA, Barkhof F, Scheltens P, Stam CJ, Smith SM, et al. Consistent resting-state networks across healthy subjects. *Proceedings of the National Academy of Sciences of the United States of America*, 103(37): 13848–13853, 2006.

Davidson RJ, Lewis DA, Alloy LB, Amaral DG, Bush G, Cohen JD, et al. Neural and behavioral substrates of mood and mood regulation. *Biological Psychiatry*, 52(6): 478–502, 2002.
Deco G and Corbetta M. The dynamical balance of the brain at rest. *Neuroscientist*, 17(1): 107–123, 2011.
Du AT, Jahng GH, Hayasaka S, Kramer JH, Rosen HJ, Gorno-Tempini ML, et al. Hypoperfusion in frontotemporal dementia and Alzheimer disease by arterial spin labeling MRI. *Neurology*, 67(7): 1215–1220, 2006.
Eslinger PJ, Moore P, Antani S, Anderson C, and Grossman M. Apathy in frontotemporal dementia: Behavioral and neuroimaging correlates. *Behavioural Neurology*, 25(2): 127–136, 2012.
Farb NA, Segal ZV, Mayberg H, Bean J, McKeon D, Fatima Z, et al. Attending to the present: Mindfulness meditation reveals distinct neural modes of self-reference. *Social Cognitive and Affective Neuroscience*, 2(4): 313–322, 2007.
Filley CM and Gross KF. Psychosis with cerebral white matter disease. *Neuropsychiatry, Neuropsychology and Behavioral Neurology*, 5(2): 119–125, 1992.
Foster NL, Heidebrink JL, Clark CM, Jagust WJ, Arnold SE, Barbas NR, et al. FDG-PET improves accuracy in distinguishing frontotemporal dementia and Alzheimer's disease. *Brain*, 130(Pt 10): 2616–2635, 2007.
Fox MD and Raichle ME. Spontaneous fluctuations in brain activity observed with functional magnetic resonance imaging. *Nature Reviews Neuroscience*, 8(9): 700–711, 2007.
Fox MD, Snyder AZ, Vincent JL, Corbetta M, Van Essen DC, and Raichle ME. The human brain is intrinsically organized into dynamic, anticorrelated functional networks. *Proceedings of the National Academy of Sciences of the United States of America*, 102(27): 9673–9678, 2005.
Freedman M, Binns MA, Black SE, Murphy C, and Stuss DT. Theory of mind and recognition of facial emotion in dementia: Challenge to current concepts. *Alzheimers Disease and Associated Disorders*, [Epub ahead of print] 2012.
Friston KJ, Holmes AP, Price CJ, Buchel C, and Worsley KJ. Multisubject fMRI studies and conjunction analyses. *NeuroImage*, 10(4): 385–396, 1999.
Friston KJ, Penny WD, and Glaser DE. Conjunction revisited. *NeuroImage*, 25(3): 661–667, 2005.
Gabel MJ, Foster NL, Heidebrink JL, Higdon R, Aizenstein HJ, Arnold SE, et al. Validation of consensus panel diagnosis in dementia. *Archives of Neurology*, 67(12): 1506–1512, 2010.
Goldberg II, Harel M, and Malach R. When the brain loses its self: Prefrontal inactivation during sensorimotor processing. *Neuron*, 50(2): 329–339, 2006.
Goodkind MS, Gyurak A, McCarthy M, Miller BL, and Levenson RW. Emotion regulation deficits in frontotemporal lobar degeneration and Alzheimer's disease. *Psychology and Aging*, 25(1): 30–37, 2010.
Gorno-Tempini ML, Hillis AE, Weintraub S, Kertesz A, Mendez M, Cappa SF, et al. Classification of primary progressive aphasia and its variants. *Neurology*, 76(11): 1006–1014, 2011.
Gregory C, Lough S, Stone V, Erzinclioglu S, Martin L, Baron-Cohen S, et al. Theory of mind in patients with frontal variant frontotemporal dementia and Alzheimer's disease: Theoretical and practical implications. *Brain*, 125(Pt 4): 752–764, 2002.
Greicius M. Resting-state functional connectivity in neuropsychiatric disorders. *Current Opinion in Neurology*, 21(4): 424–430, 2008.
Greicius MD, Krasnow B, Reiss AL, and Menon V. Functional connectivity in the resting brain: A network analysis of the default mode hypothesis. *Proceedings of the National Academy of Sciences of the United States of America*, 100(1): 253–258, 2003.
Greicius MD, Srivastava G, Reiss AL, and Menon V. Default-mode network activity distinguishes Alzheimer's disease from healthy aging: Evidence from functional MRI. *Proceedings of the National Academy of Sciences of the United States of America*, 101(13): 4637–4642, 2004.
Habas C, Kamdar N, Nguyen D, Prater K, Beckmann CF, Menon V, et al. Distinct cerebellar contributions to intrinsic connectivity networks. *Journal of Neuroscience*, 29(26): 8586–8594, 2009.
Harciarek M and Jodzio K. Neuropsychological differences between frontotemporal dementia and Alzheimer's disease: A review. *Neuropsychology Review*, 15(3): 131–145, 2005.
Himberg J, Hyvarinen A, and Esposito F. Validating the independent components of neuroimaging time series via clustering and visualization. *NeuroImage*, 22(3): 1214–1222, 2004.
Kelley WM, Macrae CN, Wyland CL, Caglar S, Inati S, and Heatherton TF. Finding the self? An event-related fMRI study. *Journal of Cognitive Neuroscience*, 14(5): 785–794, 2002.
Kertesz A, Davidson W, and Fox H. Frontal behavioral inventory: Diagnostic criteria for frontal lobe dementia. *Canadian Journal of Neurological Sciences*, 24(1): 29–36, 1997.
Kertesz A, Davidson W, McCabe P, and Munoz D. Behavioral quantitation is more sensitive than cognitive testing in frontotemporal dementia. *Alzheimers Disease and Associated Disorders*, 17(4): 223–229, 2003.
Kertesz A, Nadkarni N, Davidson W, and Thomas AW. The Frontal Behavioral Inventory in the differential diagnosis of frontotemporal dementia. *Journal of the International Neuropsychological Society*, 6(4): 460–468, 2000.
Kipps CM and Hodges JR. Theory of mind in frontotemporal dementia. *Social Neuroscience*, 1(3–4): 235–244, 2006.
Koch W, Teipel S, Mueller S, Benninghoff J, Wagner M, Bokde AL, et al. Diagnostic power of default mode network resting state fMRI in the detection of Alzheimer's disease. *Neurobiology of Aging*, 33(3): 466–478, 2012.
Krueger CE, Laluz V, Rosen HJ, Neuhaus JM, Miller BL, and Kramer JH. Double dissociation in the anatomy of socioemotional disinhibition and executive functioning in dementia. *Neuropsychology*, 25(2): 249–259, 2011.
Kumfor F, Miller L, Lah S, Hsieh S, Savage S, Hodges JR, et al. Are you really angry? The effect of intensity on facial emotion recognition in frontotemporal dementia. *Social Neuroscience*, 6(5–6): 502–514, 2011.
Laird AR, Fox PM, Eickhoff SB, Turner JA, Ray KL, McKay DR, et al. Behavioral interpretations of intrinsic connectivity networks. *Journal of Cognitive Neuroscience*, 23(12): 4022–4037, 2011.
Lavenu I, Pasquier F, Lebert F, Petit H, and Van der Linden M. Perception of emotion in frontotemporal dementia and Alzheimer disease. *Alzheimers Disease and Associated Disorders*, 13(2): 96–101, 1999.
Levenson RW and Miller BL. Loss of cells—loss of self: Frontotemporal lobar degeneration and human emotion. *Current Directions in Psychological Science*, 16(6): 289–294, 2007.
Lindau M, Almkvist O, Kushi J, Boone K, Johansson SE, Wahlund LO, et al. First symptoms – Frontotemporal dementia versus Alzheimer's disease. *Dementia and Geriatric Cognitive Disorders*, 11(5): 286–293, 2000.
Liu Y, Wang K, Yu C, He Y, Zhou Y, Liang M, et al. Regional homogeneity, functional connectivity and imaging markers of Alzheimer's disease: A review of resting-state fMRI studies. *Neuropsychologia*, 46(6): 1648–1656, 2008.
Lough S, Kipps CM, Treise C, Watson P, Blair JR, and Hodges JR. Social reasoning, emotion and empathy in frontotemporal dementia. *Neuropsychologia*, 44(6): 950–958, 2006.
Lowe MJ, Dzemidzic M, Lurito JT, Mathews VP, and Phillips MD. Correlations in low-frequency BOLD fluctuations reflect cortico-cortical connections. *NeuroImage*, 12(5): 582–587, 2000.
Lowe MJ, Mock BJ, and Sorenson JA. Functional connectivity in single and multislice echoplanar imaging using resting-state fluctuations. *NeuroImage*, 7(2): 119–132, 1998.

Mak HK, Zhang Z, Yau KK, Zhang L, Chan Q, and Chu LW. Efficacy of voxel-based morphometry with DARTEL and standard registration as imaging biomarkers in Alzheimer's disease patients and cognitively normal older adults at 3.0 Tesla MR imaging. *Journal of Alzheimers Disease*, 23(4): 655–664, 2011.

Manes F, Sahakian B, Clark L, Rogers R, Antoun N, Aitken M, et al. Decision-making processes following damage to the prefrontal cortex. *Brain*, 125(Pt 3): 624–639, 2002.

Matsuo K, Mizuno T, Yamada K, Akazawa K, Kasai T, Kondo M, et al. Cerebral white matter damage in frontotemporal dementia assessed by diffusion tensor tractography. *Neuroradiology*, 50(7): 605–611, 2008.

McIntosh AR and Lobaugh NJ. Partial least squares analysis of neuroimaging data: Applications and advances. *NeuroImage*, 23(Suppl. 1): S250–S263, 2004.

Menon V and Uddin LQ. Saliency, switching, attention and control: A network model of insula function. *Brain Structure and Function*, 214(5–6): 655–667, 2010.

Merrilees J, Dowling GA, Hubbard E, Mastick J, Ketelle R, and Miller BL. Characterization of apathy in persons with frontotemporal dementia and the impact on family caregivers. *Alzheimers Disease and Associated Disorders*, [Epub ahead of print] 2012.

Merrilees JJ and Miller BL. Long-term care of patients with frontotemporal dementia. *Journal of the American Medical Directors Association*, 4(6 Suppl.): S162–S164, 2003.

Miller BL, Seeley WW, Mychack P, Rosen HJ, Mena I, and Boone K. Neuroanatomy of the self: Evidence from patients with frontotemporal dementia. *Neurology*, 57(5): 817–821, 2001.

Minzenberg MJ, Fan J, New AS, Tang CY, and Siever LJ. Fronto-limbic dysfunction in response to facial emotion in borderline personality disorder: An event-related fMRI study. *Psychiatry Research*, 155(3): 231–243, 2007.

Morris JC. The Clinical Dementia Rating (CDR): Current version and scoring rules. *Neurology*, 43(11): 2412–2414, 1993.

Neary D, Snowden JS, Gustafson L, Passant U, Stuss D, Black S, et al. Frontotemporal lobar degeneration: A consensus on clinical diagnostic criteria. *Neurology*, 51(6): 1546–1554, 1998.

Paakki JJ, Rahko J, Long X, Moilanen I, Tervonen O, Nikkinen J, et al. Alterations in regional homogeneity of resting-state brain activity in autism spectrum disorders. *Brain Research*, 1321: 169–179, 2010.

Passarotti AM, Sweeney JA, and Pavuluri MN. Fronto-limbic dysfunction in mania pre-treatment and persistent amygdala over-activity post-treatment in pediatric bipolar disorder. *Psychopharmacology (Berl)*, 216(4): 485–499, 2011.

Pessoa L. How do emotion and motivation direct executive control? *Trends in Cognitive Sciences*, 13(4): 160–166, 2009.

Peters F, Perani D, Herholz K, Holthoff V, Beuthien-Baumann B, Sorbi S, et al. Orbitofrontal dysfunction related to both apathy and disinhibition in frontotemporal dementia. *Dementia and Geriatric Cognitive Disorders*, 21(5–6): 373–379, 2006.

Raichle ME, MacLeod AM, Snyder AZ, Powers WJ, Gusnard DA, and Shulman GL. A default mode of brain function. *Proceedings of the National Academy of Sciences of the United States of America*, 98(2): 676–682, 2001.

Rombouts SA, Barkhof F, Goekoop R, Stam CJ, and Scheltens P. Altered resting state networks in mild cognitive impairment and mild Alzheimer's disease: An fMRI study. *Human Brain Mapping*, 26(4): 231–239, 2005.

Salavert J, Gasol M, Vieta E, Cervantes A, Trampal C, and Gispert JD. Fronto-limbic dysfunction in borderline personality disorder: A 18F-FDG positron emission tomography study. *Journal of Affective Disorders*, 131(1–3): 260–267, 2011.

Sammler D, Kotz SA, Eckstein K, Ott DV, and Friederici AD. Prosody meets syntax: The role of the corpus callosum. *Brain*, 133(9): 2643–2655, 2010.

Sanfey AG, Rilling JK, Aronson JA, Nystrom LE, and Cohen JD. The neural basis of economic decision-making in the Ultimatum Game. *Science*, 300(5626): 1755–1758, 2003.

Seeley WW. Anterior insula degeneration in frontotemporal dementia. *Brain Structure and Function*, 214(5–6): 465–475, 2010.

Seeley WW, Crawford RK, Zhou J, Miller BL, and Greicius MD. Neurodegenerative diseases target large-scale human brain networks. *Neuron*, 62(1): 42–52, 2009.

Seeley WW, Menon V, Schatzberg AF, Keller J, Glover GH, Kenna H, et al. Dissociable intrinsic connectivity networks for salience processing and executive control. *Journal of Neuroscience*, 27(9): 2349–2356, 2007.

Shigenobu K, Ikeda M, Fukuhara R, Maki N, Hokoishi K, Nebu A, et al. The Stereotypy Rating Inventory for frontotemporal lobar degeneration. *Psychiatry Research*, 110(2): 175–187, 2002.

Smith SM, Fox PT, Miller KL, Glahn DC, Fox PM, Mackay CE, et al. Correspondence of the brain's functional architecture during activation and rest. *Proceedings of the National Academy of Sciences of the United States of America*, 106(31): 13040–13045, 2009.

Snowden JS, Austin NA, Sembi S, Thompson JC, Craufurd D, and Neary D. Emotion recognition in Huntington's disease and frontotemporal dementia. *Neuropsychologia*, 46(11): 2638–2649, 2008.

Snowden JS, Bathgate D, Varma A, Blackshaw A, Gibbons ZC, and Neary D. Distinct behavioural profiles in frontotemporal dementia and semantic dementia. *Journal of Neurology, Neurosurgery and Psychiatry*, 70(3): 323–332, 2001.

Snowden JS, Gibbons ZC, Blackshaw A, Doubleday E, Thompson J, Craufurd D, et al. Social cognition in frontotemporal dementia and Huntington's disease. *Neuropsychologia*, 41(6): 688–701, 2003.

Sridharan D, Levitin DJ, and Menon V. A critical role for the right fronto-insular cortex in switching between central-executive and default-mode networks. *Proceedings of the National Academy of Sciences of the United States of America*, 105(34): 12569–12574, 2008.

Sturm VE, Rosen HJ, Allison S, Miller BL, and Levenson RW. Self-conscious emotion deficits in frontotemporal lobar degeneration. *Brain*, 129(Pt 9): 2508–2516, 2006.

Thiebaut de Schotten M, Dell'Acqua F, Valabregue R, and Catani M. Monkey to human comparative anatomy of the frontal lobe association tracts. *Cortex*, 48(1): 82–96, 2012.

Werner KH, Roberts NA, Rosen HJ, Dean DL, Kramer JH, Weiner MW, et al. Emotional reactivity and emotion recognition in frontotemporal lobar degeneration. *Neurology*, 69(2): 148–155, 2007.

Wiech K, Lin CS, Brodersen KH, Bingel U, Ploner M, and Tracey I. Anterior insula integrates information about salience into perceptual decisions about pain. *Journal of Neuroscience*, 30(48): 16324–16331, 2010.

Yang X, Beason-Held L, Resnick SM, and Landman BA. Biological parametric mapping with robust and non-parametric statistics. *NeuroImage*, 57(2): 423–430, 2011.

Yeterian EH, Pandya DN, Tomaiuolo F, and Petrides M. The cortical connectivity of the prefrontal cortex in the monkey brain. *Cortex*, 48(1): 58–81, 2012.

Zamboni G, Huey ED, Krueger F, Nichelli PF, and Grafman J. Apathy and disinhibition in frontotemporal dementia: Insights into their neural correlates. *Neurology*, 71(10): 736–742, 2008.

Zang Y, Jiang T, Lu Y, He Y, and Tian L. Regional homogeneity approach to fMRI data analysis. *NeuroImage*, 22(1): 394–400, 2004.

Zhang Y, Schuff N, Du AT, Rosen HJ, Kramer JH, Gorno-Tempini ML, et al. White matter damage in frontotemporal

dementia and Alzheimer's disease measured by diffusion MRI. *Brain*, 132(Pt 9): 2579–2592, 2009.

Zhou J, Greicius MD, Gennatas ED, Growdon ME, Jang JY, Rabinovici GD, et al. Divergent network connectivity changes in behavioural variant frontotemporal dementia and Alzheimer's disease. *Brain*, 133(Pt 5): 1352–1367, 2010.

Zou Q, Wu CW, Stein EA, Zang Y, and Yang Y. Static and dynamic characteristics of cerebral blood flow during the resting state. *NeuroImage*, 48(3): 515–524, 2009.

Zou QH, Zhu CZ, Yang Y, Zuo XN, Long XY, Cao QJ, et al. An improved approach to detection of amplitude of low-frequency fluctuation (ALFF) for resting-state fMRI: Fractional ALFF. *Journal of Neuroscience Methods*, 172(1): 137–141, 2008.